Electronic Supplementary Material (ESI) for Soft Matter.

Supplementary Information for:

Photoinduced repetitive separation of the supramolecular assembly composed of amphiphilic diarylethene mixture

Seiya Sakakibara, Hajime Yotsuji, Kenji Higashiguchi* and Kenji Matsuda*

Department of Synthetic Chemistry and Biological Chemistry, Graduate School of Engineering, Kyoto University, Katsura, Nishikyo-ku, Kyoto 615-8510, Japan

Contents

1. Additional figures

1.1 Chromatograms.

1.2 Phase transition and absorption spectra.

1.3 Optical images.

1.4 TEM images.

1.5 DLS measurement.

2. Movie captions

References

1. Additional figures

1.1 Chromatograms.

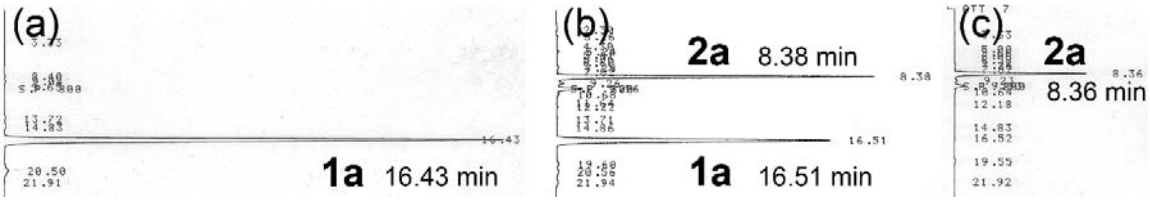

Fig. S1 Examples of HPLC chromatograms of white-turbid suspensions containing (a) **1**:**2** = 1:0, (b) 0.5:0.5, and (c) 0:1.

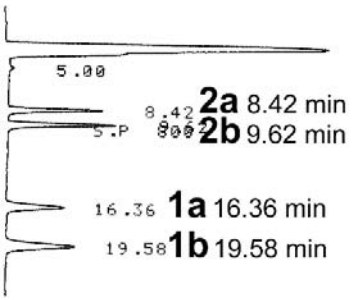

Fig. S2 An example of HPLC chromatogram of suspension upon irradiation with 365 nm light for 120 s to the suspension containing **1**:**2** = 0.50:0.50. The photoisomerization yield to the closed-ring isomer was obtained as 66%. The chromatogram corresponds to Figs. S5f, S6f, and Table S1 (entry f).

1.2 Phase transition and absorption spectra.

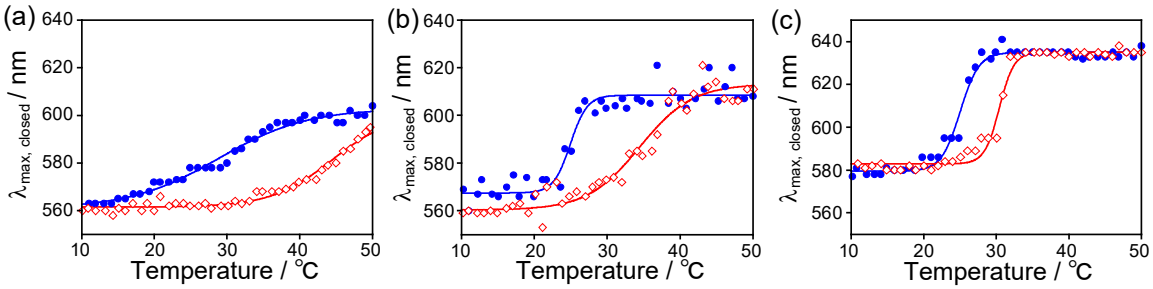

Fig. S3 The hysteresis of absorption maximum against temperature for the mixed suspensions with different composition ratios. The composition ratio of **1**:**2**, photoisomerization yield, and hysteresis were (a) 0.50:0.50, 60%, 16 °C, (b) 1:0, 56%, 10 °C, and (c) 0:1, 58%, 6 °C, respectively. The cooling and heating rate was 1.0 °C min^{-1}. Blue filled circles and red open diamonds are cooling and subsequent heating, respectively.

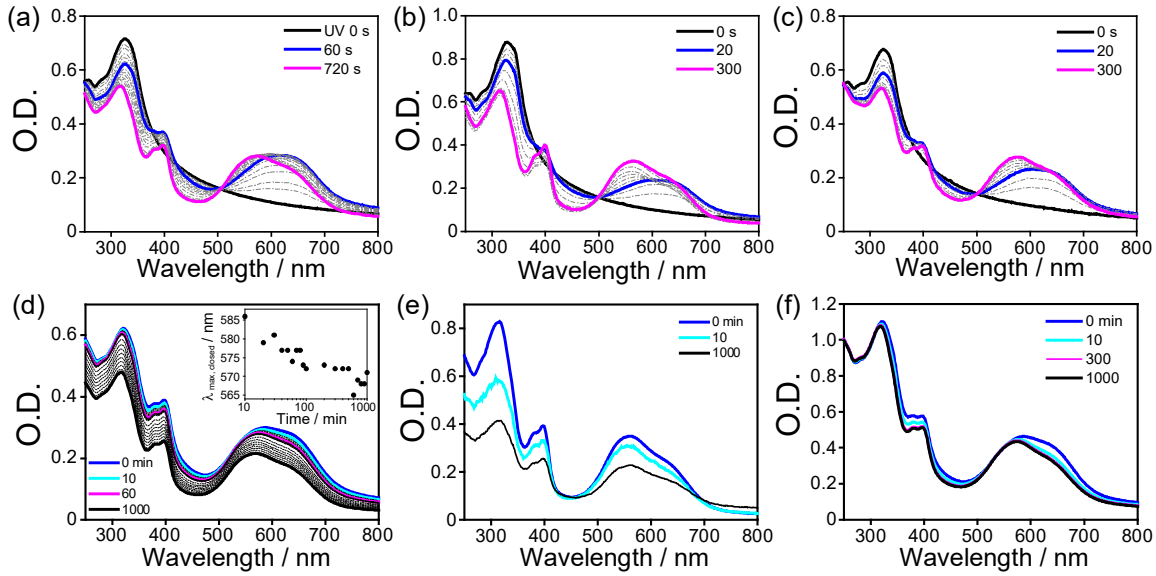

Fig. S4 The spectral shift (a-c) during continuous irradiation with UV (365 nm) light and (d-f) upon standing in the dark for the sample irradiated with UV (365 nm) light for 90 s. (a, d) **1**:**2** = 0.49:0.51, (b, e) 1:0, and (c, f) 0:1. The time for reorientation was ca. 100 min in the mixed assembly as shown in the inset of (d). The assembly composed of pure **1** and **2** required <10 min for the reorientation forming H-aggregate.

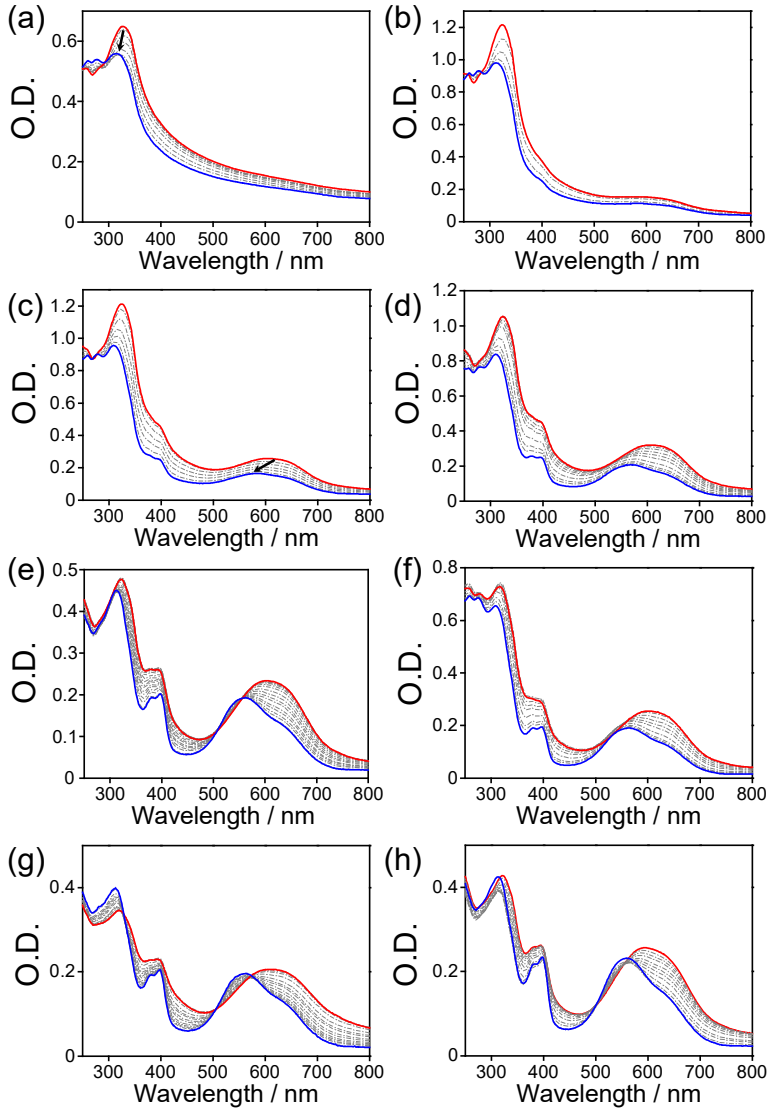

Fig. S5 The change in absorption spectra of the suspension containing **1**:**2** = 0.5:0.5 (see Table S1) by cooling at 1 °C min^{-1} at various photoisomerization yield. (a) 0%, (b) 11%, (c) 25%, (d) 44%, (e) 54%, (f) 66%, (g) 83%, and (h) 84%. Red solid lines correspond to (a) 20, (b) 30, (c, d) 40, and (e-h) 60 °C, respectively, and blue solid lines correspond to (a-e) 0 °C and (f-h) 5°C, respectively. The spectral change at (e) 54% is identical to Fig. 2a in the main text.

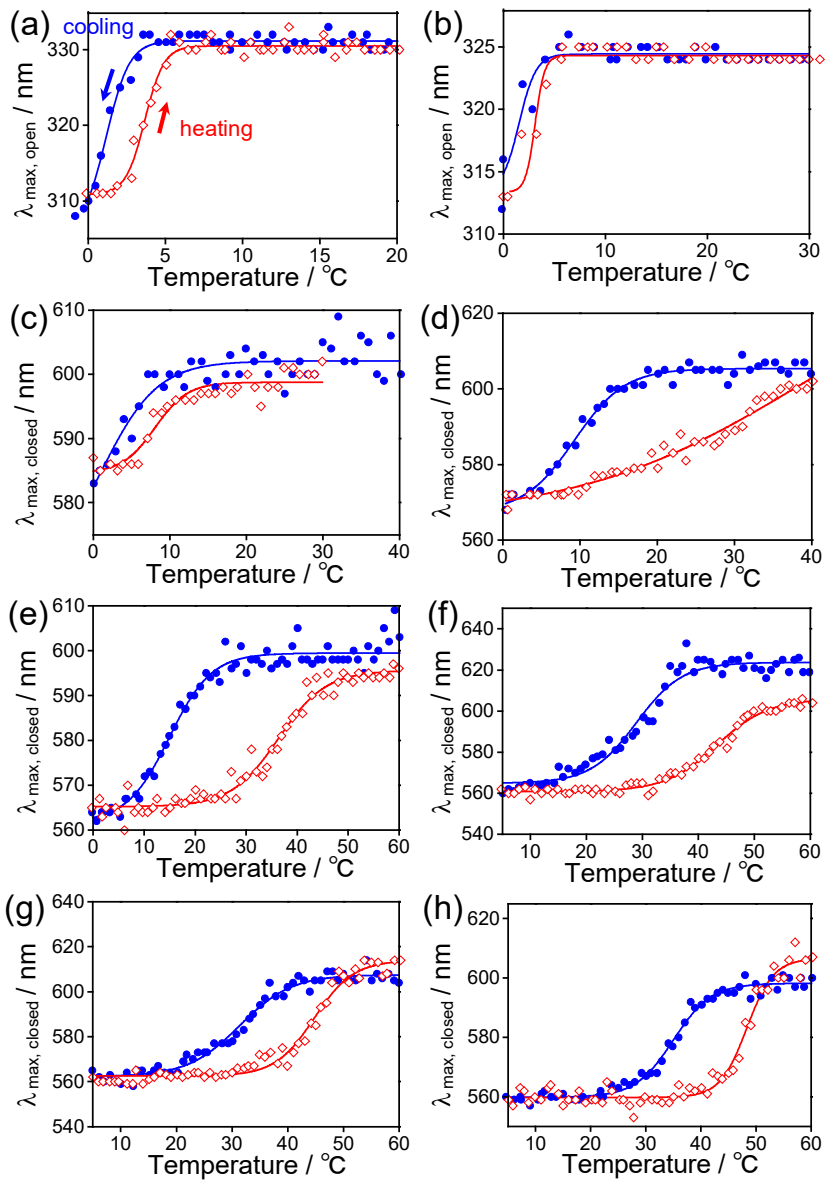

Fig. S6 The change in absorption maxima at the visible range under temperature control corresponding to Fig. S5. Absorption maximum of the open-ring isomer (ca. 320 nm) was monitored for (a) and (b) because of the low photoisomerization yield. Blue filled circles and red open diamonds are cooling and subsequent heating, respectively. The change at (e) 54% is identical to Fig. 2b in the main text.

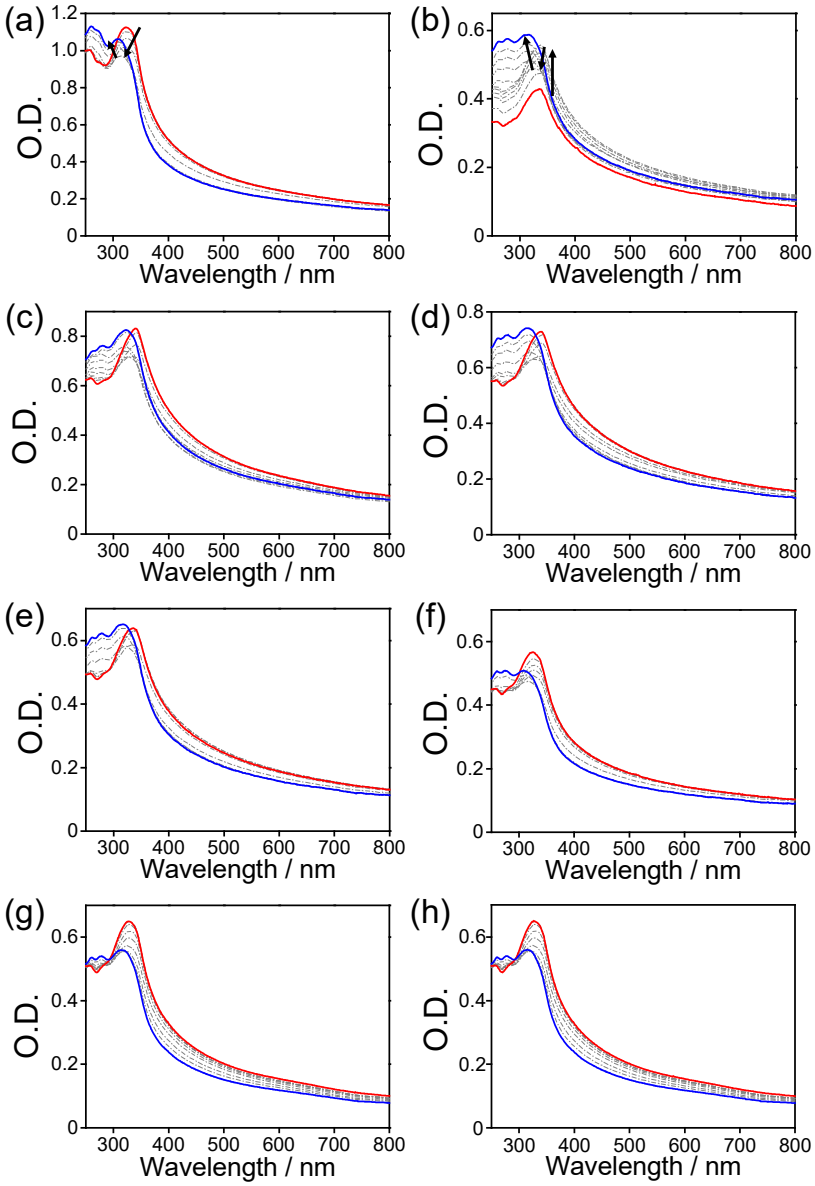

Fig. S7 The change in absorption spectra of the colorless suspension (0% of photoisomerization yield) containing **1** and **2** by cooling for 1 °C min^{-1} with various composition ratios **1**:**2**. (a) **1**:**2** = 0:1, (b) 0.06:0.94, (c) 0.11:0.89, (d) 0.20:0.80, (e) 0.30:0.70, (f) 0.36:0.64, (g) 0.54:0.46, and (h) 0.56:0.44. Red and blue solid lines correspond to 20 and 0 °C, respectively.

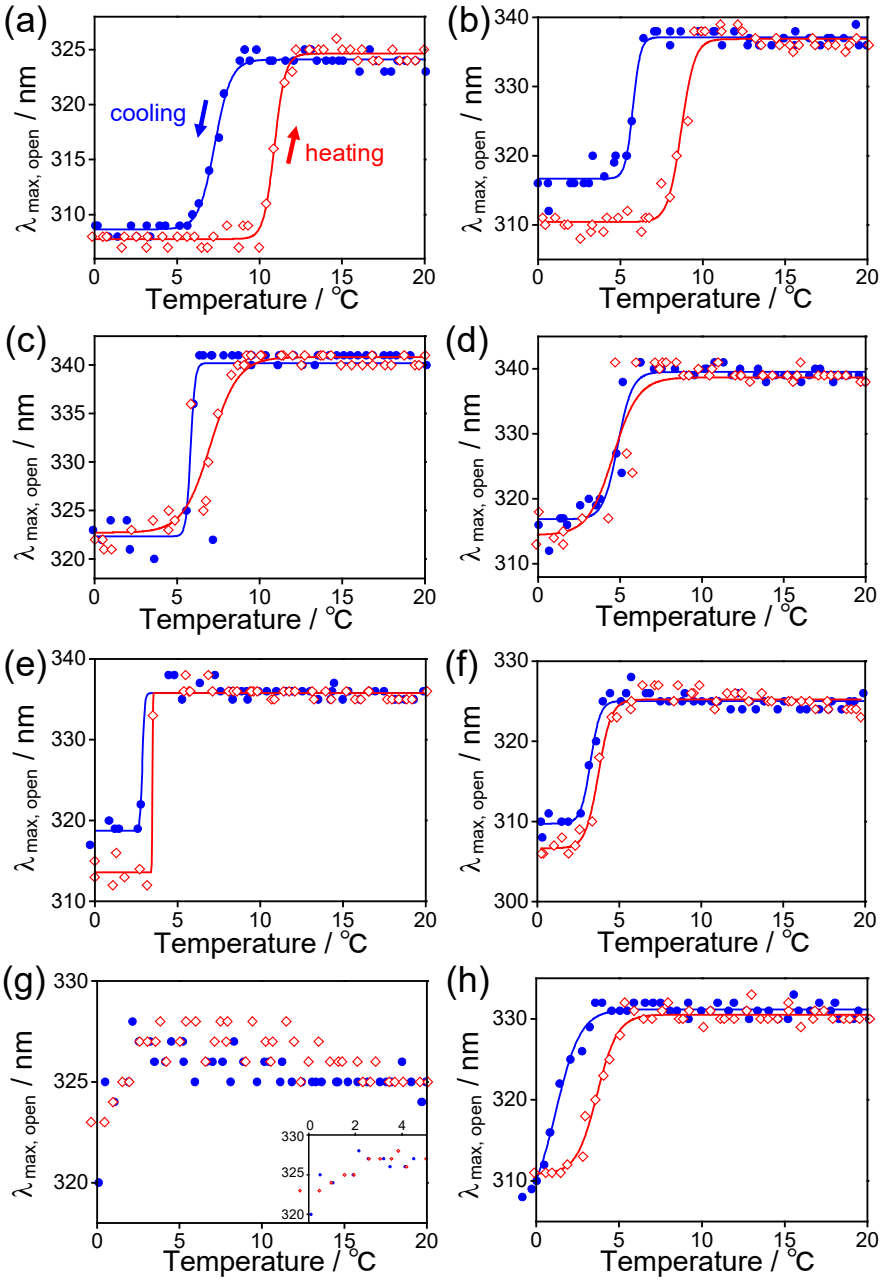

Fig. S8 The change in absorption maxima of the open-ring isomer under temperature control corresponding to Fig. S7. For panel (g), the transition point was not determined by the fitting curve.

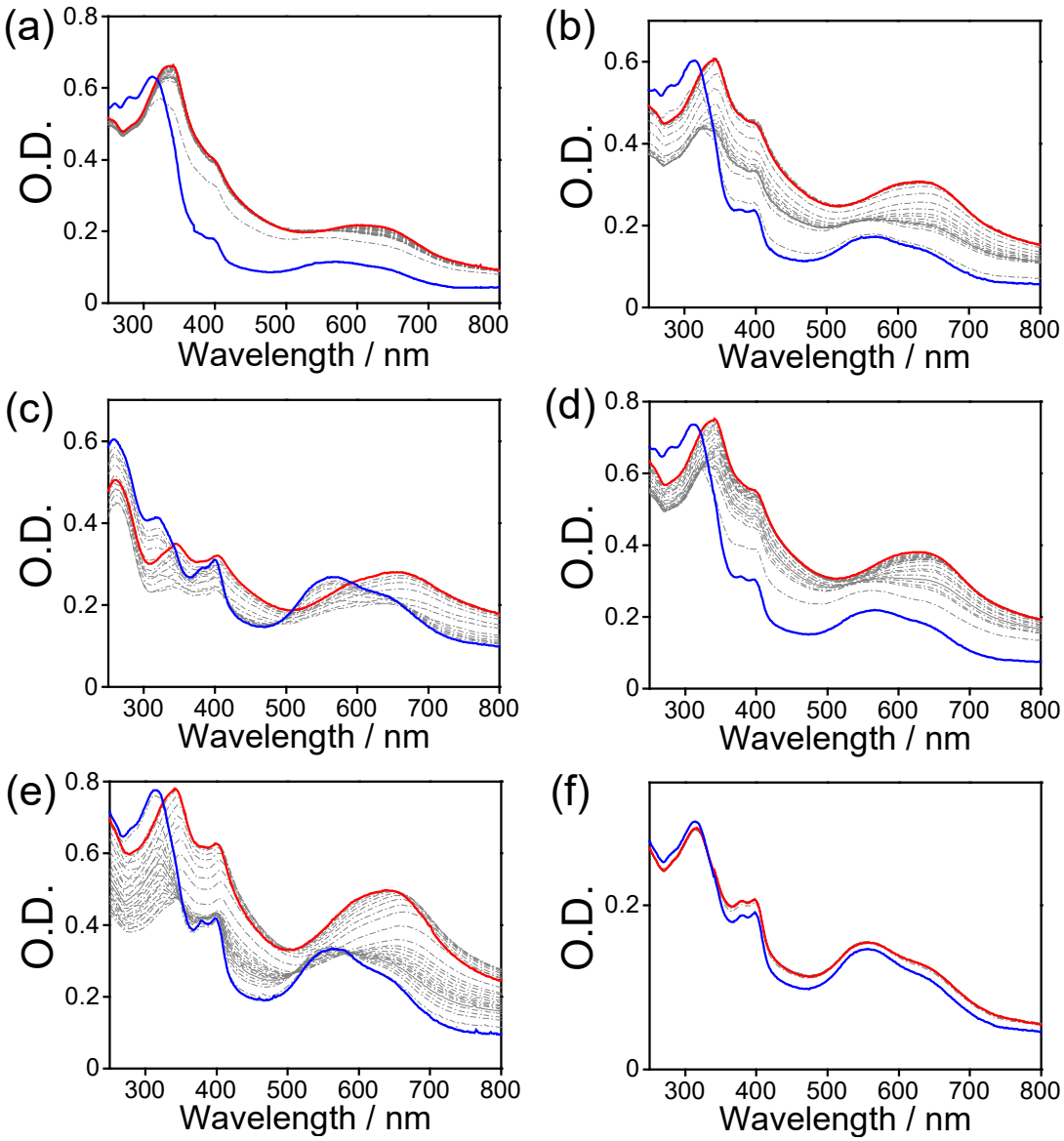

Fig. S9 The change in absorption spectra of the suspension containing excess of **1** by cooling for 1 °C min^{-1} at various photoisomerization yield. The composition ratio of **1**:**2** and photoisomerization yield were (a) 0.83:0.17, 19%, (b) 0.83:0.17, 23%, (c) 0.75:0.25, 85%, (d) 0.70:0.30, 37%, (e) 0.70:0.30, 23%, and (f) 0.69:0.31, 46%, respectively.

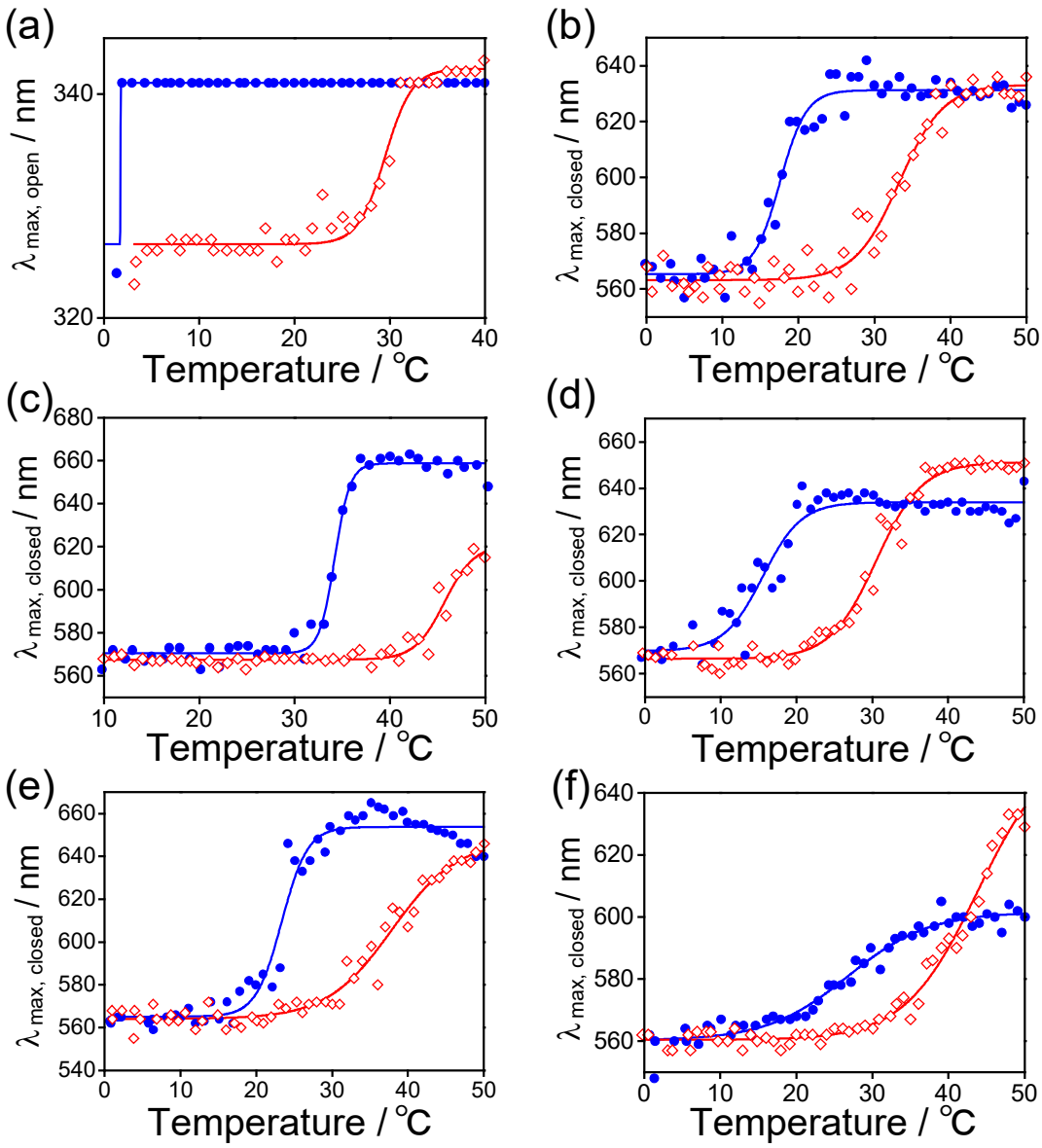

Fig. S10 The change in absorption maxima under temperature control corresponding to Fig. S9. Absorption maximum of the open-ring isomer (ca. 320 nm) was monitored in (a).

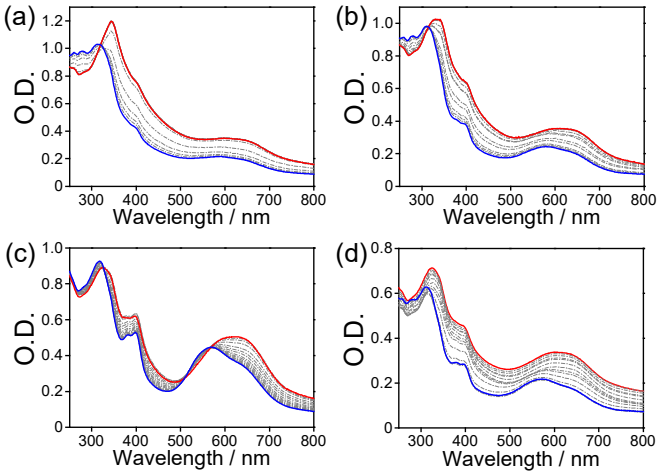

Fig. S11 The change in absorption spectra of the suspension containing excess of **2** by cooling for 1 °C min^{-1} at various photoisomerization yield. The composition ratio **1**:**2** and photoisomerization yield were (a) 0.33:0.67, 20%, (b) 0.33:0.67, 35%, (c) 0.36:0.64, 74%, and (d) 0.23:0.77, 32%, respectively.

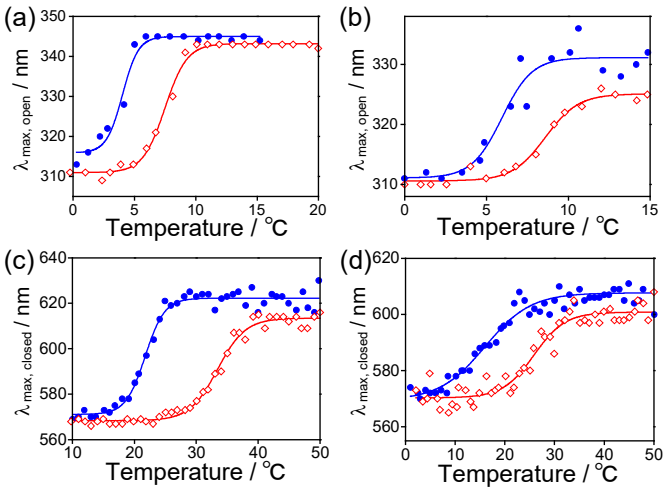

Fig. S12 The change in absorption maxima under temperature control corresponding to Fig. S11. Absorption maximum of the open-ring isomer (ca. 320 nm) was monitored in (a) and (b).

Table S1. The contents corresponding to Figs. 6a, S5, and S6.

	1a / %	**2a** / %	**1b** / %	**2b** / %	Composition ratio **1**:**2**	Photoisomerization yield / %	*T* / °C
(a)	55.7	44.3	0	0	0.56:0.44	0	2.7
(b)	43.2	45.7	4.7	6.4	0.48:0.52	11	2.9
(c)	36.5	38.2	11.9	13.4	0.48:0.52	25	5.1
(d)	27.1	29.0	20.4	23.5	0.48:0.52	44	14
(e)	22.0	24.5	25.2	28.3	0.47:0.53	54	30
(f)	16.5	17.7	34.0	31.8	0.50:0.50	66	35
(g)	7.3	9.9	40.8	42.0	0.48:0.52	83	40
(h)	6.1	10.0	42.2	41.7	0.48:0.52	84	43

Table S2. The contents corresponding to Figs. 6b, S7, and S8.

	Composition ratio **1**:**2**	Photoisomerization yield / %	*T* / °C
(a)	0:1	0	7.5
(b)	0.06:0.94	0	7.1
(c)	0.11:0.89	0	5.6
(d)	0.20:0.80	0	4.8
(e)	0.30:0.70	0	3.6
(f)	0.36:0.64	0	3.3
(g)	0.54:0.46	0	N/A
(h)	0.56:0.44	0	2.7

Table S3. The contents corresponding to Figs. S9 and S11.

	1a / %	**2a** / %	**1b** / %	**2b** / %	Composition ratio **1**:**2**	Photoisomerization yield / %	*T* / °C
S9-(a)	67.5	13.9	15.9	2.7	0.83:0.17	19	14
S9-(b)	64.4	12.6	18.9	4.1	0.83:0.17	23	24
S9-(c)	11.3	3.8	63.5	21.4	0.75:0.25	85	40
S9-(d)	44.4	18.2	25.9	11.5	0.70:0.30	37	24
S9-(e)	54.7	22.2	15.4	7.7	0.70:0.30	23	29
S9-(f)	37.0	17.1	32.1	13.8	0.69:0.31	46	35
S11-(a)	27.9	52.4	5.9	13.8	0.33:0.67	20	5.4
S11-(b)	22.2	43.3	10.5	24.0	0.33:0.67	35	7.2
S11-(c)	8.7	27.0	17.6	46.7	0.36:0.64	74	27
S11-(d)	15.9	7.3	51.9	24.9	0.23:0.77	32	22

Table S4. The contents corresponding to Fig. 6a.[S1]

Composition ratio **1**:**2**	Photoisomerization yield / %	*T* / °C	Composition ratio **1**:**2**	Photoisomerization yield / %	*T* / °C
1:0	25	10	0:1	0	7.8
1:0	56	27	0:1	2	9.3
1:0	76	37	0:1	43	25
1:0	96	46	0:1	58	28
			0:1	76	36
			0:1	98	39

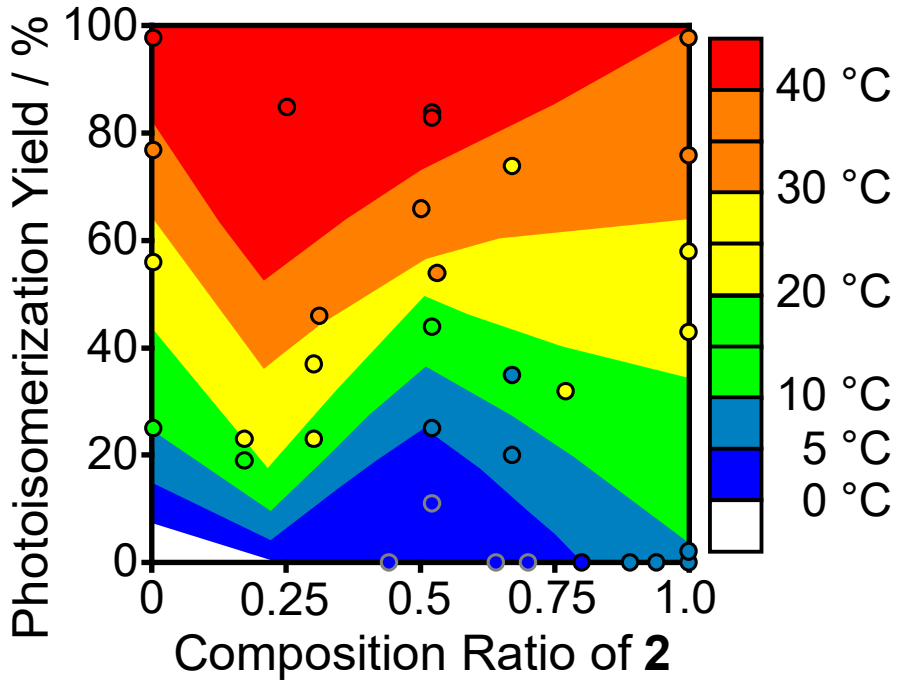

Fig. S13 The two-dimensional heat map showing LCST for both composition ratio and photoisomerization yield at various temperature. The region shown in dark blue and white is identical to Fig. 6c in the main text.

1.2.1 behavior of pure 1 and 2.

The spectral change of pure **1** and **2** under temperature control were measured. Area of absorption spectrum, which was obtained by integration of optical density (O.D.) in the range between 250 and 800 nm, was used because of the precipitation (see below). The O.D. change is mainly responded to the change in size and shape of the supramolecular assembly.

The change in area of integrated O.D. were different between pure **1** and pure **2** (Fig. S14). The well-colored (96% of **1b**) microsphere broke into fibers and the fiber

shrunk to sphere (<100 nm) upon cooling and heating, respectively. As a result, the assembly adhered to cuvette as shown in Fig. S14c (inset). Therefore, the area decreased steeply in both the cooling and heating processes. On the other hand, pure **2** kept the shape along with the phase transition.[S1] Therefore the area change was small and reversible.

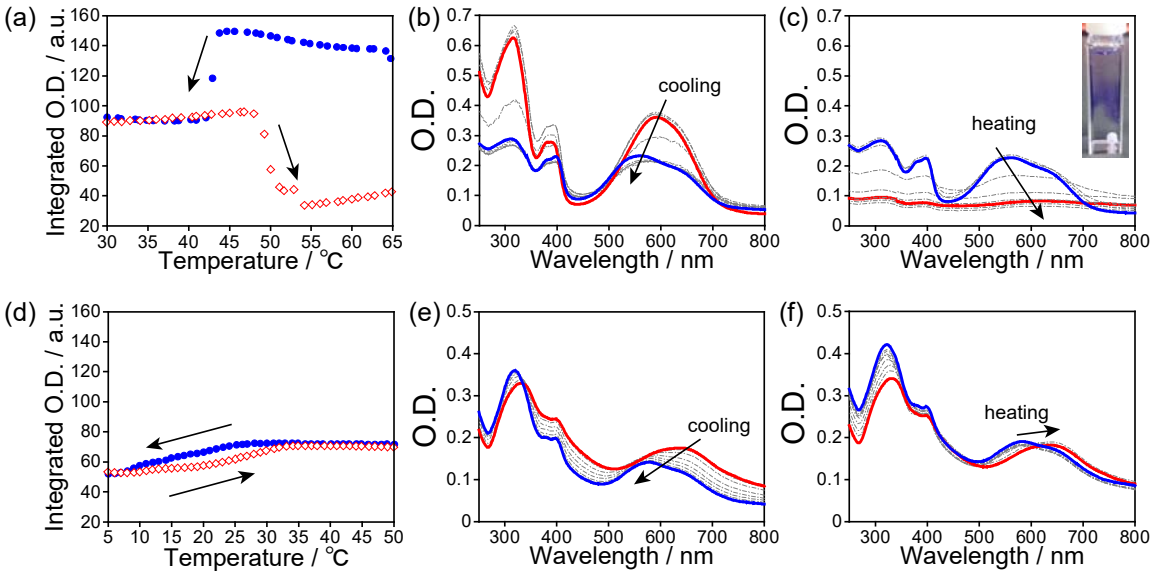

Fig. S14 The change in scattering of the suspension composed of (a-c) pure **1** and (d-f) **2**. The photoisomerization yield of **1** and **2** were 96 and 43%, respectively. (a, d) Change in area obtained by the integration of O.D. at the range of 250 to 800 nm. Blue filled circles and red open diamonds are cooling and subsequent heating, respectively. Inset of (c) shows an example of adhesion of ester-linked **1** to the cuvette. The precipitation was not observed in amide-linked **2**. (b, c, e, f) The corresponding change in absorption spectra upon (b, e) cooling and (c, f) subsequent heating.

1.2.2 mixing of the two compounds.

According to our previous report, when the photoisomerization yields of diarylethenes **1** and **2** are similar, the LCST points are considered to be rather similar. In this case, it is difficult to distinguish whether the phase transition is one- or two-step to judge the homogeneity of the mixture. Therefore, we have prepared the mixture from the diarylethenes **1** and **2** with different photoisomerization yields. In this case, difference in the LCST points of **1** and **2** gets larger, so that the distinction gets easier.

Respective solutions of **1** and **2** in acetonitrile (1.0 mg mL^{-1}) were individually irradiated with UV light and the solutions of **1** and **2** with different photoisomerization yields (66 and 13% for **1** and **2**, respectively) were prepared. The expected transition temperatures were 32 and 12 °C for **1** and **2**, respectively. Two types of suspensions having the same content (**1a**:**1b**:**2a**:**2b** = 17:33:43:7) were prepared as follows: method (i), a suspension was prepared from the acetonitrile solution mixed in advance (360 μL, **1**:**2** = 50:50) and subsequent addition of water (4.0 mL). The resulting suspension contained 0.36 mg of the diarylethenes in 4.4 mL of the mixed solvent; method (ii), two suspensions (0.18 mg of the diarylethene in 2.2 mL of the mixed solvent) prepared individually from the acetonitrile solutions of **1** and **2** were simply added into the cuvette. The concentration was completely the same as (i).

In the case of (i), the change appeared as smooth one-step curve and the O.D. recovered by heating (Figs. S15a-c). Therefore, **1** and **2** were mixed homogeneously in the assembly. In contrast, two-step phase transition was observed in (ii), which indicates individual phase transitions of pure **1** (24 °C) and **2** (12 °C) (Fig. S15d). Additionally, the O.D. decreased upon both cooling and heating periods, which was similar to pure **1**, as

shown in Figs. S15e and f. These behaviors were different from the suspension (i). Thus, homogeneity of **1** and **2** in the supramolecular assembly was confirmed.

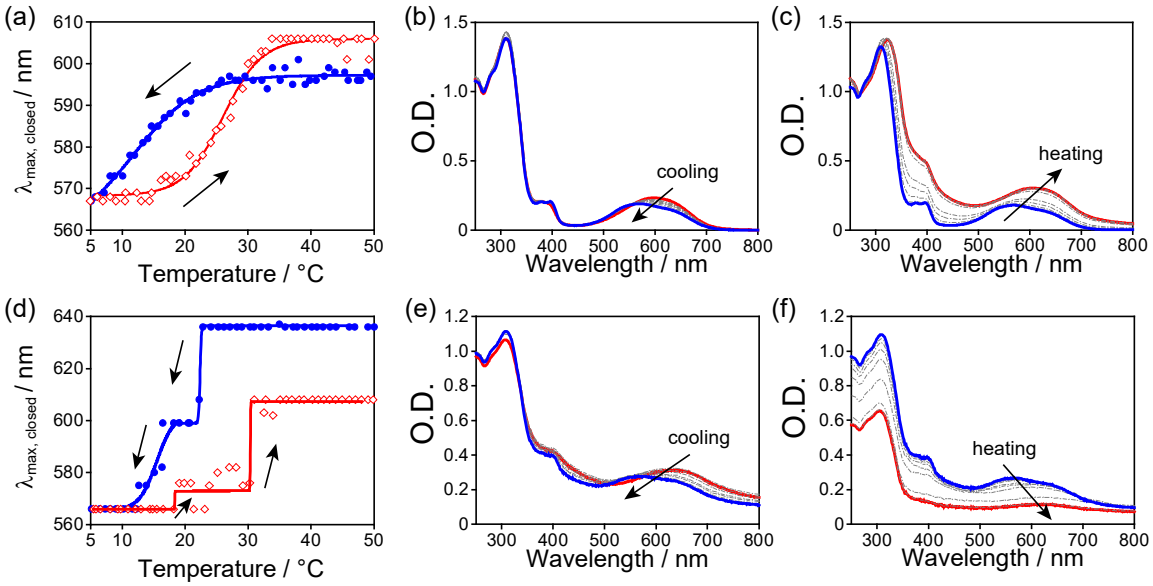

Fig. S15 The change in (a, d) absorption maxima and (b, c, e, f) absorption spectra of the suspension containing **1a**:**1b**:**2a**:**2b** = 17:33:43:7 prepared by (a-c) the method (i) and (d-f) method (ii). The spectral shift in (d) was fitted using two types of different sigmoidal curves.

1.3 Optical images.

The morphological transformation of supramolecular assembly composed of **1**:**2** = 0.81:0.19 is shown in Fig. S16. The colorless microsphere turned blue upon long (6 min) irradiation with UV light at 20 °C (Figs. S16a and b). In this irradiation condition, the mixture of **1**:**2** = 0.5:0.5 showed complete transformation at 5 °C, so that the photoisomerization ratio is estimated to be ca. 40-50%. Therefore, the sample is considered to be in the hydrated state judging from the heat map (Fig. S13), but the morphological change was not observed without standing in the dark probably due to slow reorientation described in the main text. Subsequently, the colored microsphere gradually collapsed upon cooling to 5 °C in the dark (Figs. S16c-e). The assembly disappeared upon irradiation with visible light within 10 s (Figs. S16f and g). The morphological change was similar to the behavior of pure **1** regardless of the presence of **2**.

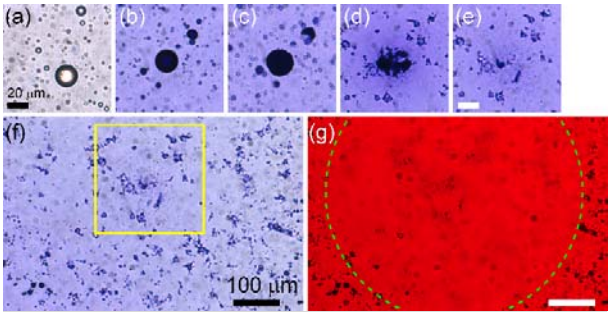

Fig. S16 The morphological change of the supramolecular assembly composed of **1**:**2** = 0.81:0.19. (a) The initial state, (b) UV irradiation for 6 min at 20 °C, (c) subsequent cooling in the dark to 5 °C for 1.7 min, (d) 14 min, and (e) 25 min. A yellow square in the reduced image (f) corresponds to (e). (g) Disappearance of supramolecular assembly upon irradiation with visible (546 nm) light for 10 s at 5 °C. A dashed green circle shows the region of photoirradiation.

The morphological change of the assembly composed of **1**:**2** = 0.38:0.62 is shown in Fig. S17. The assembly showed diameter change upon irradiation with UV light in the center of field of view even at 5 °C. (Figs. S17a-e). In contrast, flake-like structures were observed at periphery region, where relatively weak UV light was illuminated (Fig. S17f). The obtained flake-like structure showed decoloration without deformation upon subsequent irradiation with visible light at 0 °C (Figs. S17g-i). On the other hand, the flake shrunk rapidly by heating to 40 °C without photoirradiation (Figs. S17j-l). The behaviors were almost the same as pure **2**.[S1]

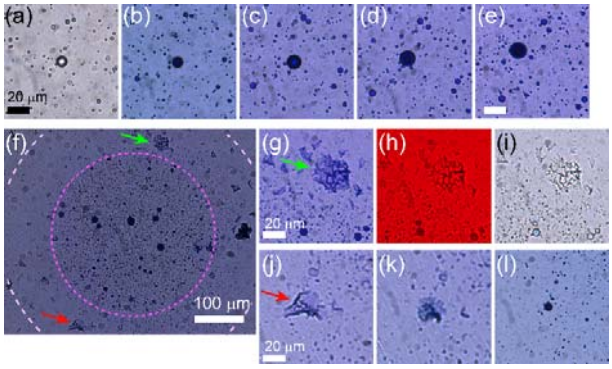

Fig. S17 The morphological transformation of the supramolecular assembly composed of **1**:**2** = 0.38:0.62. (a-e) The size expansion under UV light for 23 min at 5 °C. (f) The reduced image. (g-i) Decoloration of sheet structure without deformation upon irradiation with visible light at 0 °C. (j-l) Deformation of the sheet to sphere without photoirradiation by heating from 0 to 40 °C.

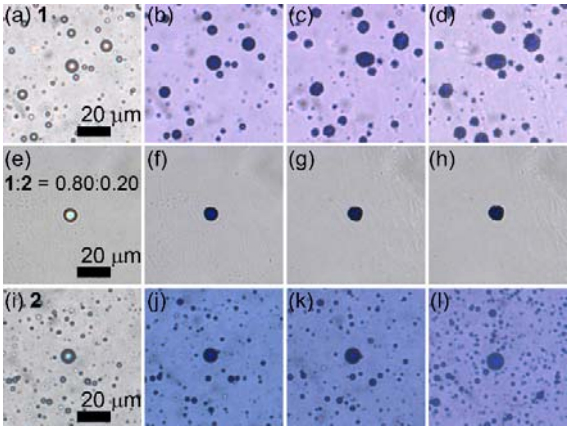

Fig. S18 The behavior of supramolecular assembly upon irradiation with UV light and standing in the dark at 5 °C for (a-d) pure **1**, (e-h) **1**:**2** = 0.80:0.20 and (e-h) **2**. Photoinduced LCST transition to the hydrated state was observed in all cases, whereas the division was not observed despite employing the same photoillumination method.

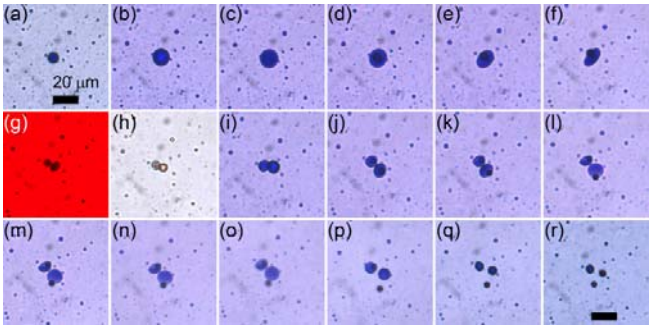

Fig. S19 The division of the supramolecular assembly composed of **1**:**2** = 0.5:0.5 by long (1 min) irradiation with UV light at 5 °C. (a-b) Irradiation with UV light, (c-f) standing in the dark, (g) irradiation with visible light, (h-i) second irradiation with UV light, (j-o) standing in the dark, and (p-r) heating to 20 °C. Large sparse structure was obtained compared to short (10 s) irradiation shown in Fig. 5 in the main text because the region having high photoisomerization yield became large. Heating was also usable to the separation. The photoirradiation was carried out without ND filter (see Fig. S20)

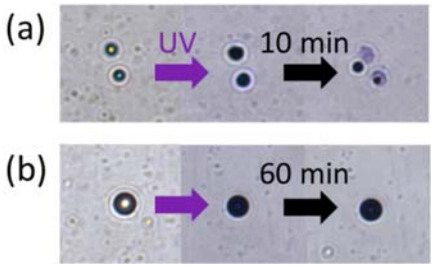

Fig. S20 The effect of light intensity and irradiation time examined by the same setup with Fig. S19. (a) The small sparse structures were generated by irradiation with UV light for 4 min through ND4 (1/4) filter and standing in the dark for 10 min at 5 °C. (b) The division was not observed even after standing in the dark for 60 min at 5 °C after irradiation with UV light for 16 min through ND16 (1/16) filter. The total amount of photon was almost the same in (a), (b), and Fig. S19. In the case of (b), light intensity was weak and the irradiation time was long, so that the diffusion of the closed-ring isomer occurred and the separation is considered to be suppressed.

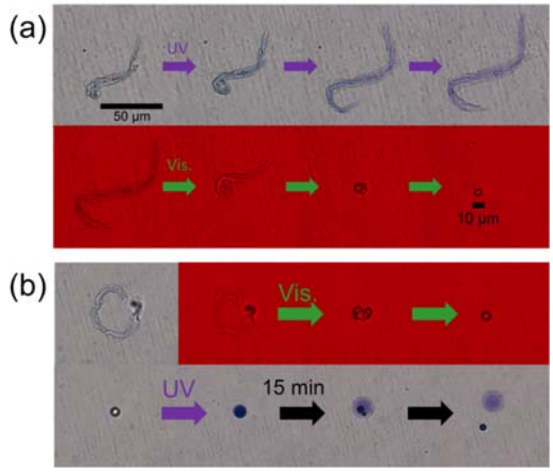

Fig. S21 The morphological transformation started from the hydrated state at 5 °C. (a) Elongation and subsequent shrinking upon irradiation with UV and visible lights, respectively. (b) Shrinking upon irradiation with visible light and subsequent division. The assembly was prepared from the acetonitrile solution, whose composition ratio and photoisomerization yield were **1**:**2** = 0.50:0.50 and 22%, respectively.

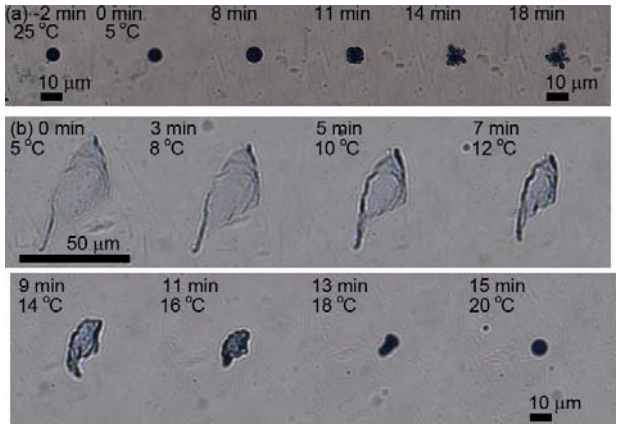

Fig. S22. The morphological change of the supramolecular assembly composed of **1**:**2** = 0.5:0.5 under (a) cooling and (b) heating. (a) The division of colored sphere upon irradiation with UV light out for 60 s at 25 °C and standing in the dark at 5 °C. (b) The shrinking of sheet-like structure having 22% of photoisomerization yield from 5 to 20 °C.

1.4 TEM images.

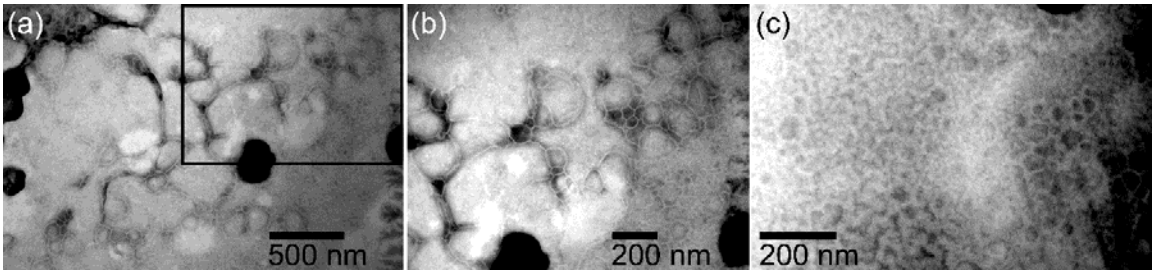

Fig. S23 The supramolecular architectures composed of **1**:**2** = 0.5:0.5 upon irradiation with UV (365 nm) light for 60 s. (a) The sufficiently aged network structure and (b) the expanded image. (c) The intermediate structure between the network and coacervate.

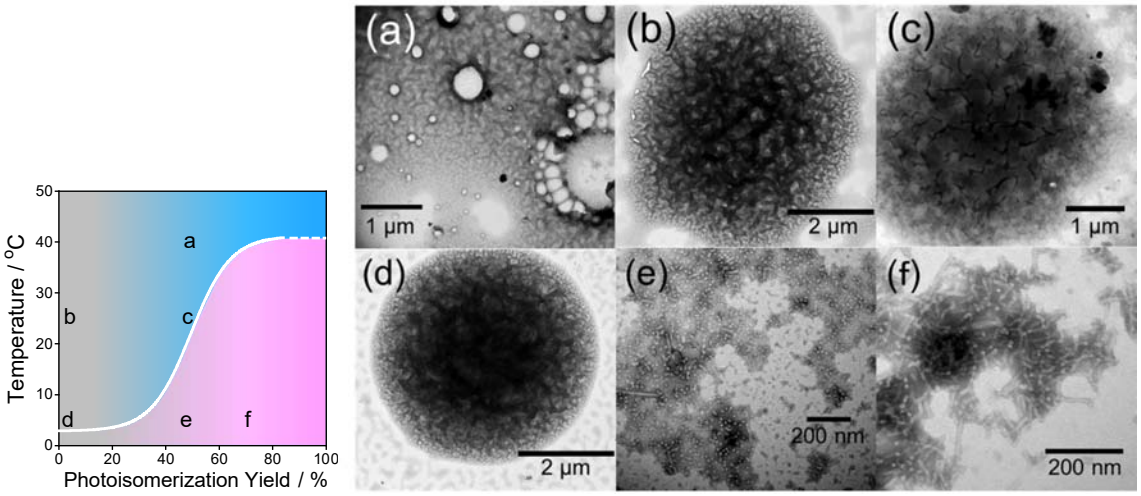

Fig. S24 TEM images of the supramolecular architectures composed of **1**:**2** = 0.5:0.5 at various temperature and photoisomerization yield.

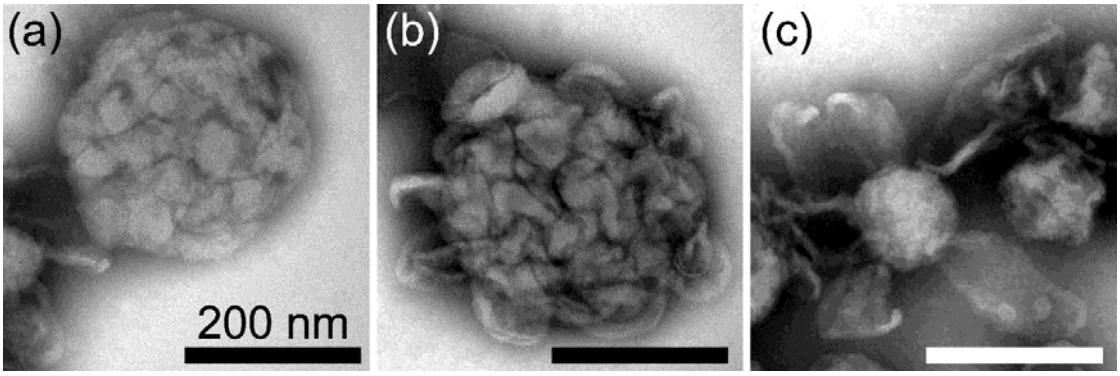

Fig. S25 Exfoilation of the folded bilayers composed of mixture of the open-ring isomers (**1a**:**2a** = 0.25:0.75). (a) Tightly folded, (b) slightly exfoliated, and (c) exfoliated structures. The corresponding structure is shown in Fig. 7d in the main text.

1.5 DLS measurement.

Particle size distribution was measured on a DLS instrument (Malvern Zetasizer μV) equipped with 830 nm diode laser as a light source, using a fixed angle (90°) at room temperature. The aqueous suspensions containing **1**:**2** = 0.5:0.5, pure **1**, and **2** were prepared as 1.0×10^{-3} M concentration. The size distributions of supramolecular assembly were determined using volume-weighted calculation by assuming no influence of viscosity, refractive index, and nanostructure between sphere and anisotropic shapes shown by TEM. Thus, the change of autocorrelation function is also shown.

The mixture showed intermediate behavior for the diameter change between pure **1** and **2**. The diameters of initial colorless sphere were almost the same. The reversible change in diameter, which was observed upon irradiation with UV and visible lights, was observed in all cases. The amount of diameter change of the mixture was between pure **1** and **2** (Fig. S25).

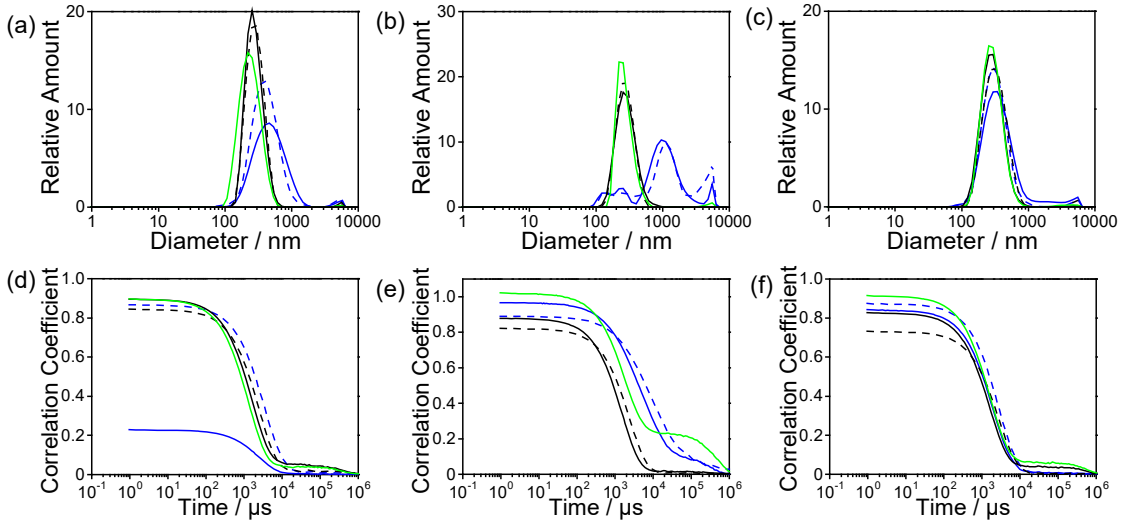

Fig. S26 (a-c) Change in volume size distribution and (d-f) autocorrelation function of (a, d) **1**:**2** = 0.5:0.5, (b, e) **1**, and (c, f) **2**. Green, blue, and black are initial (the open-ring isomer), 365 nm-irradiated (70 % of photoisomerization yield), and 578 nm-irradiated suspension (the open-ring isomer), respectively. Solid and dashed lines indicate 20 and 5 °C, respectively.

2. Movie captions

The field of view of all movies was 290 × 217 μm.

Movie S1. Separation of the supramolecular assembly composed of **1**:**2** = 0.5:0.5 by repetitive irradiation with UV light from top of the precipitated microsphere at 5 °C (see Fig. 3) by 410-fold speed of reproduction for 9750 s. The operation was as follows: cooling (3 min), first irradiation with UV light (10 s), standing in the dark (47 min), second UV-irradiation (10 s), the standing (28 min), third UV-irradiation (10 s), the standing (14 min), fourth UV-irradiation (20 s), the standing (50 min), fifth UV-irradiation (20 s), the standing (20 min), and irradiation with visible light (50 s).

Movie S2. Separation of microspheres composed of **1**:**2** = 0.5:0.5 by repetitive irradiation with UV and visible lights from top of the precipitated microsphere at 5 °C (see Fig. 5) by 250-fold speed of reproduction for 2040 s. The operation was as follows: cooling (3 min), first irradiation with UV light (10 s), standing in the dark (15 min), first irradiation with visible light (20 s), interval (15 s), second UV-irradiation (20 s), the standing (15 min), and second visible light-irradiation (20 s).

References

(S1) H. Yotsuji, K. Higashiguchi, R. Sato, Y. Shigeta and K. Matsuda, *Chem. Eur. J.*, 2017, **23**, 15059-15066.